Topic：AI and Knowledge Based Software Engineering

A Modified Segmentation Approach for Synthetic Aperture Radar Images on Level Set

Peng Qiangqiang, Zhao Long
Science and Technology on Aircraft Control Laboratory, Beihang University, Beijing 100191, China
Email: magicbirds@vip.qq.com, flylong@buaa.edu.cn

***Abstract*—In this paper, we propose a method towards unsupervised segmentation of synthetic aperture radar (SAR) image for segmentation of homogeneous regions. The SAR amplitude image is modeled by Rayleigh distribution. Moreover, in order to avoid geometric topology variations, the curve evolution is implemented via level sets. In addition, a new energy function is proposed, which is more objective and robust for the segmentation purpose. During the curve evolution, a convex factor is considered to guarantee the regularity of the region boundary. Finally, a novel termination criterion of the evolution of energy function is designed. And then, the effectiveness of our method is demonstrated on real SAR images.**

***Index Terms*—Synthetic Aperture Radar Imagery, Segmentation, Active Contours, Level Set**

I. INTRODUCTION

Segmentation of SAR images is a fundamental process in automatic interpretation of image. An increasing attention is paid on SAR since it can exhibit the unique ability of acquiring images under all weather conditions and all time, which can be crucial complementary of classical optical sensors. However, SAR image segmentation is known as a challenge problem due to the presence of speckle, which can be modeled as a strong multiplicative noise. The speckle results in a large variation of the backscatter across neighbor pixels within the homogeneous region. Local filtering and clustering-based approaches such as the Canny edge detector [1], k-means algorithm and mean shift algorithm [2-4] are some general method. And they possess a simple and convenient scheme. The dependence of the neighbor pixels value can result in incorrect segmentations of strong speckled regions. Region growing [5-10] has also been used in segmentation of SAR images. However, they have their limitations. Furthermore, a speckle reducing technique is essential, such schemes [11-14], mostly adopted local operations. As a result, the lack of robust and edge deterioration is committed. Heat diffusion equation [15] employs multi-scale anisotropic smoothing of the posterior probability matrixes to remove the impacts of speckle and to preserve important structure information. Recently, a number of active contours have been proposed for segmentation of SAR images [16-23]. The contour is iteratively deformed to locate the boundary of a region that is guided by a statistical criterion. The scheme improves the traditional snake-balloon and similar ratio filter method. The classical active contour models have several limitations, since the image is processed on a set of points. Hence, the geometric topology variation is difficult to represent. Furthermore, the errors that depend on the representation can be significantly amplified during evolution.

In this paper, we use active curves evolution via level set method to segment SAR images and Rayleigh-homogeneous regions. Level set has a significant advantage of variations in the geometric topology of curves. The topic of this study focuses on proposing energy function, decreasing iterations and setting termination criterion.

The remainder of this paper is organized as follows. In section II, the energy function and its modified form are given and the convex factor is considered in the evolution equation. In section III, the stability of the evolution process is proved. In section IV, the whole scheme of our algorithm is presented, including a termination criterion for the evolution of curves. In section V, we show the experimental results of our method on real images, which demonstrate the effectiveness of our method. Conclusions are drawn in section VI.

II. DESCRIPTION OF MODEL

Let $I(x)$ be the SAR segmented amplitude image and Ω be the domain defined by the given image $I(x)$. The goal of the segmentation process is to derive a partition of the image domain from the image $I(x)$, i.e. , a family with N subsets of Ω such that they are piece wisely disjoint, and cover all image domains. $R_i \cap R_j|_{\forall i \neq j} = \varnothing$ and $\cup_{i=1}^{N} R_i = \Omega$. Each region is homogeneous with respect to some statistical characteristics, i.e., a family of prespecified probability distributions $P(I|\alpha)$, where α is the parameter of the distribution. We assume that the probability models of regions may differ from each other.

In the case of a SAR amplitude image, we model the image in each region R_i ($i \in (1,2,\cdots,N)$), by a Rayleigh distribution as follows,

doi:10.4304/jsw.8.5.1168-1173

$$P_{R_i}(I(x)) = \frac{I(x)}{\sigma^2}\exp\left(-I(x)^2/2\sigma^2\right), \quad (1)$$

where σ is the parameter of the distribution, and *I(x)* is the intensity of image I on location x. The image in each region R_i is therefore classified by its parameter σ_i. We obtain of the region under a prior distribution as,

$$\sigma_i = 2E_i(x)/\sqrt{2\pi}, (i = (1,2,\cdots,N)), \quad (2)$$

$E_i(x)$ is estimated by the average value of *I(x)* inside a region R. Hence, we can take,

$$E_i(\mathrm{x}) = \int_{R_i} I(x)dx \Big/ \int_{R_i} dx, \quad (3)$$

Assuming that *I(x)* is independent of *I(y)* for $x \neq y$. The problem of segmentation consists of finding the family of regions $\hat{R}$, which maximizes the likelihood,

$$\hat{R} = \arg\max_{\Re} \ell(\Re \mid I) = \arg\max_{\Re} \prod_{i=1}^{N} (\prod_{x\in R_i} P_{\sigma_i}(I(x))), \quad (4)$$

Without loss of generality, the number of sub-regions is set to two. Considering the smoothness of region contour, the energy function can be written as,

$$\begin{aligned}\hat{F}(x) = 2\mu\oint_R ds - (\lambda_1\int_R \log(P_{\sigma_1}(I(x)))dx \\ + \lambda_2\int_R \log(P_{\sigma_2}(I(x)))dx)\end{aligned}, \quad (5)$$

To solve the problem of minimizing the energy function $F(x)$ by curve evolution in the case of two regions, a partial differential equation is established [24], $\frac{d\vec{\gamma}}{dt} = -\frac{\partial F}{\partial \vec{\gamma}}$, where $\vec{\gamma}$ is a closed planar curve. This function indicates that the energy function is descending with the curve evolution. Following Euler-Lagrange equation and some algebraic manipulations, the curve motion equation is obtained,

$$\begin{aligned}\frac{d\vec{\gamma}}{dt} = 2\mu\kappa_{\vec{\gamma}}\vec{n}_{\vec{\gamma}} + \lambda_1\log(P_{\sigma_1}(I(x)))\vec{n}_{\vec{\gamma}}, \\ - \lambda_2\log(P_{\sigma_2}(I(x)))\vec{n}_{\vec{\gamma}}\end{aligned} \quad (6)$$

where $\kappa_{\vec{\gamma}}$ is the curvature of curve $\vec{\gamma}$, and $\vec{n}_{\vec{\gamma}}$ is the unit normal to curve $\vec{\gamma}$. The above motion equation has a simple intuitive interpretation. There are three terms involved in the evolution process, the smoothing term, the interior statistics term, and the exterior statistics term, respectively.

It is difficult to process geometric topology variations by explicit representation. In contrast, level-set based approaches allow geometric topology to change in a natural way. They can be implemented by stable numerical schemes.

The energy function with level-set can be described as follows,

$$\begin{aligned}\hat{F}(\phi) = \mu\int_R |\nabla H(\phi(x))|dx \\ + \lambda_1\int_R -\log(P_{\sigma_1}(I(x)))H(\phi(x))dx \\ + \lambda_2\int_R -\log(P_{\sigma_2}(I(x)))H(-\phi(x))dx\end{aligned}, \quad (7)$$

Let the exterior normal be represented by $\vec{n}_{\vec{\gamma}} = \nabla\phi/|\nabla\phi|$, then the level-set based motion equation is turned into,

$$\begin{aligned}\frac{\partial\phi(x,t)}{\partial t} = \mu\kappa_{\vec{\gamma}}\cdot\frac{\nabla\phi(x,t)}{|\nabla\phi(x,t)|} \\ + \lambda_1\log(P_{\sigma_1}(I(x))) - \lambda_2\log(P_{\sigma_2}(I(x)))\end{aligned}, \quad (8)$$

Shuai et al. proposed a modified energy function, which aims at overcoming a local minimum problem of the regular energy function [23]. It can be described as follows,

$$\begin{aligned}F(\phi) = \mu\int_R |\nabla H(\phi(x))|dx \\ + \lambda_1\int_R -\log(P_{\sigma_1}(I(x))\phi(x)H(\phi(x)+\alpha)dx \\ + \lambda_2\int_R -\log(P_{\sigma_2}(I(x))(-\phi(x))H(-\phi(x)+\alpha)dx\end{aligned}, \quad (9)$$

Then the level-set based motion equation is,

$$\begin{aligned}\frac{\partial\phi(x,t)}{\partial t} = \mu\kappa_{\vec{\gamma}}\cdot\frac{\nabla\phi(x,t)}{|\nabla\phi(x,t)|} \\ + \lambda_1\log(P_{\sigma_1}(I(x)))H(\phi(x)+\alpha) \\ - \lambda_2\log(P_{\sigma_2}(I(x)))H(-\phi(x)+\alpha)\end{aligned}, \quad (10)$$

where μ is an arbitrary positive value, $H(\phi)$ is the 1-D Heaviside function.

The minimization of $F(\phi)$ with regard to ϕ results in a level set function whose zero level set becomes the boundary of the segmentation result. However, in the computer graphics, the amplitude SAR image is representing a rectangular grid of pixels. The zero level region boundaries are difficult to detect in pixels. For convenience, we take the zero cross level set region as the boundary. The functional (9) is a modified functional (7) by multiplying $\phi(x)$ in the energy functional and substituting the Heaviside function by a shifted Heaviside function. This modification benefits two aspects. The energy functional could reflect the level set changes By multiplying $\phi(x)$. The shifted Heaviside function could compensate for the loss of the zero level boundaries in the rectangular grid pixels representation. In the pixels image, the region boundary is no longer just the set where $\phi(x) = 0$, and moreover, the boundary can be located in the set where $\phi(x) \in [-\alpha, \alpha]$, where α is the shifted value of the shifted Heaviside function.

However, the energy functional (9) may have a defect for segmentation. For the reason that the principal factor for the segmentation result is the region boundaries. Therefore, the region beyond its boundary is less important as the near boundary ones during the evolution process. Otherwise, the curve evolution is driven by the differentiation between the interior and exterior statistics term and the effect near the boundary of the region is more intensive than that in the interior region.

In this paper, we substitute the factors $\phi(x)$ and $-\phi(x)$ into the second and third terms of the functional (9) by new factors $W(\phi(x)) = \frac{2}{\pi}\arctan(\phi(x))$ and $W(-\phi(x)) = \frac{2}{\pi}\arctan(-\phi(x))$. The energy function is transformed into,

$$\begin{aligned}\widetilde{F}(\phi) &= \mu\int_R |\nabla H(\phi(x))|dx \\ &+ \lambda_1\int_R -\log(P_{\sigma_1}(I(x))W(\phi(x))H(\phi(x)+\alpha)dx \\ &+ \lambda_2\int_R -\log(P_{\sigma_2}(I(x))W(-\phi(x))H(-\phi(x)+\alpha)dx\end{aligned} \quad , (11)$$

In function (11), the contribution of the region, where the absolute value of level is large, decreases than functional (9). Meanwhile, the energy of the interior region has similar values. Therefore, this modification is more suitable for the segmentation purpose.

The Equation (10) is obtained by the gradient descent energy functional (9) . Zhu et al. [24] have calculated that the gradient of the energy function with respect to any point on the region boundary by Euler-Lagrange equation and Green's theorem.

$$\begin{aligned}&E = \iint_R f(x,y)dxdy \\ &\Rightarrow \quad \frac{\delta E}{\delta v} = f(x,y)\vec{n}_{(x,y)} = -\frac{dv}{dt}\end{aligned}, \quad (12)$$

where v is the boundary point of region R and $\vec{n}_{(x,y)} = (\dot{y},-\dot{x})$ is the normal along the boundary. Since the left-hand side of the boundary is the inside region area. $\vec{n}_{(x,y)} = (\dot{y},-\dot{x})$ is actually the exterior norm. It is obviously independent of the local convexity.

We can write equation (12) as follows,

$$E = \int_0^l L(x(s),\dot{x}(s),y(s),\dot{y}(s))ds\,, \quad (13)$$

By means of Euler-Lagrange equation, we turn the first term of the function (9) into the explicit representation form,

$$\begin{aligned}&\mu\int_R |\nabla H(\phi(x))|dx \\ &\Rightarrow \quad \mu\oint_{\partial R} d\ell = \mu\int_0^l \sqrt{\dot{x}(s)^2+\dot{y}(s)^2}\,ds\end{aligned}, \quad (14)$$

where ℓ is the arc length of the region boundary. Then we can obtain,

$$\begin{aligned}\frac{\delta E}{\delta x} &= \frac{\partial L}{\partial x} - \frac{d}{ds}\frac{\partial L}{\partial \dot{x}} = \frac{\ddot{y}\dot{x}-\ddot{x}\dot{y}}{(\dot{x}^2+\dot{y}^2)^{3/2}}\dot{y} \\ \frac{\delta E}{\delta y} &= \frac{\partial L}{\partial y} - \frac{d}{ds}\frac{\partial L}{\partial \dot{y}} = \frac{\ddot{y}\dot{x}-\ddot{x}\dot{y}}{(\dot{x}^2+\dot{y}^2)^{3/2}}(-\dot{x})\end{aligned}, \quad (15)$$

Thus it follows,

$$\frac{\delta E}{\delta v} = sign(\ddot{y}\dot{x}-\ddot{x}\dot{y})\kappa\vec{n}_{(x,y)}\,, \quad (16)$$

where $\kappa = \frac{|\ddot{y}\dot{x}-\ddot{x}\dot{y}|}{(\dot{x}^2+\dot{y}^2)^{3/2}}$ is a local curvature, $sign(\cdot)$ is defined as follows,

$$sign(x) = \begin{cases} 1 & x>0 \\ 0 & x=0 \\ -1 & x<0 \end{cases}, \quad (17)$$

We find that,

$$sign(\ddot{y}\dot{x}-\ddot{x}\dot{y}) = \begin{cases} 1 & if\ the\ local\ boundary \\ & is\ convex \\ -1 & else \end{cases}, \quad (18)$$

As a result, the function derivative of an integral along the boundary is correlated with both the curvature value and the local convexity. However, when utilizing the above conclusion to get the equation (10), the local convexity of the boundaries is ignored.

Now, we can calculate the motion equation to minimize the energy function (12) with addition of the local convexity,

$$\begin{aligned}\frac{d\phi(x,t)}{dt} &= -\frac{\delta\widetilde{F}}{\delta\phi} = -\mu\kappa(x,t)\cdot convex(x,t)\frac{\nabla\phi(x,t)}{|\nabla\phi(x,t)|} \\ &+ (\lambda_1\log(P_{\sigma_1}(I(x)))H(\phi(x,t)+\alpha)(\frac{2}{\pi(1+\phi^2(x,t))}) \\ &- (\lambda_2\log(P_{\sigma_2}(I(x)))H(-\phi(x,t)+\alpha)(\frac{2}{\pi(1+\phi^2(x,t))})\end{aligned} \quad , (19)$$

where $convex(\cdot)$ is true, if the local boundary is convex. In what follows, we use ϕ to denote $\phi(x,t)$.

III. STABILITY ANALYSIS OF THE BOUNDARY EVOLUTION

We define a Lyapunov function V by $V = \phi^2/2$, and take the time derivation of V along the trajectory of the (19). Then, by using (19), we obtain,

$$\begin{aligned}\dot{V} &= \phi[-\mu\kappa(x,t)\cdot convex(x,t)\frac{\nabla\phi}{|\nabla\phi|} \\ &+ \lambda_1\log(P_{\sigma_1}(I(x)))H(\phi+\alpha)(\frac{2}{\pi(1+\phi^2)}) \\ &- \lambda_2\log(P_{\sigma_2}(I(x)))H(-\phi+\alpha)(\frac{2}{\pi(1+\phi^2)})]\end{aligned} \quad , (20)$$

Firstly, let us analyze the effect of the convexity for the evolution stability. If the local level set is convex, namely, $convex(x,t)=1$. We can obtain $-\mu\kappa(x,t)\cdot convex(x,t)\le 0$. If the local level set is concave, which means $convex(x,t)=-1$, thus, $-\mu\kappa(x,t)\cdot convex(x,t)\ge 0$. We can find that, for the case of convex, the first term of the equation (20) would enhance the stability of the evolution process. In contrast, for the case of concave, the opposite effect would arise. However, if $\dot{V}>0$, which means the evolution process is unstable, thus $|\phi|'>0$. It implies that the $|\phi|$ would increase and the local level set would evolve into convex. As a result, the evolution process would turn into the convex case. Therefore, for convenience, we ignored the concave situation in the following analysis.

(1) When $\phi\ge\alpha\ge 0$, $H(\phi+\alpha)=1$ and $H(-\phi+\alpha)=0$, thus we have,

$$\begin{aligned}\dot{V} &= \phi(-\mu\kappa(x,t)\cdot convex(x,t) \\ &+ \lambda_1\log(P_{\sigma_1}(I(x)))(\frac{2}{\pi(1+\phi^2)})\end{aligned}, \quad (21)$$

where $\kappa(x,t)\ge 0$, $\frac{2}{\pi(1+\phi^2)}>0$ and $P_{\sigma_1}(I(x)\in[0,1]\Rightarrow\log(P_{\sigma_1}(I(x))\le 0$.

Since the local level set is supposed to be convex, namely, $convex(x,t)=1$. We can obtain $\dot{V}\le 0$.

(2) When $\alpha > \phi > 0$, $H(\phi + \alpha) = 1$ and $H(-\phi + \alpha) = 1$, we have,

$$\begin{aligned} \dot{V} &= \phi(-\mu\kappa(x,t) \cdot convex(x,t) \\ &+ \lambda_1 \log(P_{\sigma_1}(I(x)))(\frac{2}{\pi(1+\phi^2)}) \\ &- \lambda_2 \log(P_{\sigma_2}(I(x)))(\frac{2}{\pi(1+\phi^2)})) \end{aligned} \quad , \quad (22)$$

Then we suppose that $\log(P(I(x) \mid \hat{\sigma}_1)) < \log(P(I(x) \mid \hat{\sigma}_2))$, which implies the pixel x is less distributed under the parameter in salient region than that with background region. And then it is easy to guarantee that $\dot{V} < 0$. In other words, the level set function ϕ evolutes towards the more distributed region, when it is in a less distributed one.

For $\log(P(I(x) \mid \hat{\sigma}_1)) > \log(P(I(x) \mid \hat{\sigma}_2))$, we can not guarantee $\dot{V} < 0$. For the case of $\dot{V} > 0$, ϕ would increase. One can easily find that there must exist a positive value $\varepsilon \le \alpha$, if $\phi > \varepsilon$, we can guarantee $\dot{V} < 0$. In other word, the evolution will turn into a stable process.

For the situation of $\phi < 0$, similar result can be obtained.

Hence, the evolution process of the level set achieves a global stability, and the minimum ϕ will converge at the interval $[-\alpha - \tau, a + \varsigma]$, where τ and ς are a finite positive value.

IV. Segmentation Framework

A. Initialization ofLevel Se tsFunction

The proposed model can achieve the global minimum regardless of the initialization, which is proved in section 3. This implies that the evolution can start with any initial ϕ function, and the same result ϕ can be obtained when the evolution process becomes stable.

B. Curve Evolution

To minimize the energy function $\hat{F}(\phi)$, the following two steps are iteratively implemented. At first, keeping ϕ fixed, we compute the parameters $\hat{\sigma}$, i.e.

$$\hat{\sigma}_i = \arg\max_{\sigma} \prod_{x \in R_i} P(\sigma \mid I(x)), \quad i = (1,2,\cdots,N), \quad (23)$$

where, we choose $\hat{\sigma}_i$ by means of function (2). The other step is keeping all the $\hat{\sigma}$ fixed, and minimizing $\hat{F}(\phi)$ with respect to ϕ. Hereafter, the modified curve evolution equation is obtained,

$$\begin{aligned} \frac{d\phi(x,t)}{dt} &= -\frac{\delta\tilde{F}}{\delta\phi} = -\mu\kappa(x,t) \cdot convex(x,t) \frac{\nabla\phi(x,t)}{|\nabla\phi(x,t)|} \\ &+ (\lambda_1 \log(P_{\hat{\sigma}_1}(I(x) \mid \hat{\sigma}_1) H(\phi(x,t) + \alpha) \\ &(\frac{2}{\pi(1+\phi^2(x,t))}) - (\lambda_2 \log(P_{\hat{\sigma}_2}(I(x) \mid \hat{\sigma}_2) \\ &H(-\phi(x,t) + \alpha)(\frac{2}{\pi(1+\phi^2(x,t))}) \end{aligned} \quad , \quad (24)$$

where $\hat{\sigma}_1$ denotes the parameter of an object salient region, $\hat{\sigma}_2$ denotes the parameter of the background region, κ is the curvature of the level sets. It can be calculated by central difference approximations,

One can start with initial level set function, and then we obtain the segmentation result till the evolution achieves a stable state.

C. Termination Criterion

The existing termination criteria for level-set based SAR image segmentation have some drawbacks. For instance, a termination criterion based on the comparison between any properties of the current and previous steps is not appropriate, because this would be likely to converge to a local minimum.

Since the segmentation is implemented by a curve evolution, the termination criterion would be set with respect to the evolution itself. Therefore, we define that when the evolution equation achieves a steady state, the segmentation would be terminated.

During the evolution process, $\Delta\phi$ is iteratively calculated by (24), which is the control signal for the evolution. Since the state variable ϕ would converge to a certain interval, the control signal would decay to zero. As a result, the evolution process would be terminated, when the control signal is small enough.

We define the absolute mean (*AM*) to evaluate the magnitude of the control signal as follows,

$$mean(|\Delta\phi|) = 1/N \cdot \sum |\Delta\phi(r)|, \quad (25)$$

where N denotes the amount of pixels in the object image. Every $\Delta\phi(r)$ would achieve a convergence. As a result, the *AM* would converge to a certain interval $[-\beta_1, \beta_2]$, where β_i is a non-negative value close to zero.

To enhance the robustness of the termination criterion with respect of *AM*, one can average a sequence of *AM*, and then calculate the mean of *AM* sequence(*MAMS*),

$$MAMS = \sum_{t=t_i}^{t_i+sn-1} AM(t)/sn, \quad (26)$$

where sn is the length of *AM* sequence. One can just measure the *MAMS* every time step and terminate the algorithm if the *MAMS* becomes very small. If the value of *MAMS* is smaller than the preset threshold, the evolution will be terminated and the rough SAR image segmentation result will be obtained.

D. Merging Regions

An energy variance function is defined as follows,

$$\begin{aligned} \Delta E = &\iint_{R_1 \cap R_2} \log(P(I(x) \mid \sigma_{R_1 \cup R_2})) - \iint_{R_1} \log(P(I(x) \mid \sigma_{R_1})) \\ &- \iint_{R_2} \log(P(I(x) \mid \sigma_{R_2})) + \varsigma \end{aligned} \quad , \quad (27)$$

where $\sigma_{R_1}, \sigma_{R_2}, \sigma_{R_1 \cup R_2}$ are the parameters of region $R_1, R_2, R_1 \cup R_2$ respectively, and ς is a nonnegative value. If $\Delta E < 0$, then merging R_1 and R_2.

V. Experimental Results

In this section, our method is demonstrated on real SAR images. During implementation, we generally choose the

parameters as follows, $\alpha = 2, \lambda_1 = 0.2, \lambda_2 = 0.2, \varsigma = 100, \mu = 0.6$ and the threshold of *MAMS* is *0.02.* We simply initialize the level set function having a value of 1 with 30×30 pixels in the left top of the SAR image and the rest region having a value of -1.

In Fig. 1, we compare the segmentations of the proposed method with the method in [23]. It can be seen that, without multiplying a convex check factor, the previous SAR image segmentation method based on the level set in [23] performs worse on the regularity of the result. Furthermore, our method is much more robust, since the level sets of the region close to the boundary have high absolute value.

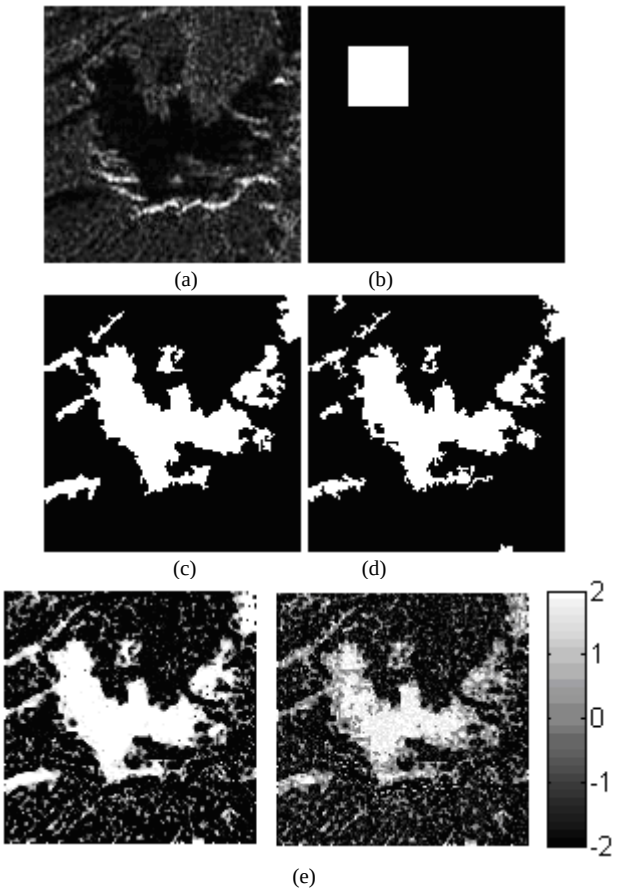

Figure 1. Fig. 1 Comparison between the segmentation results of our method and the method proposed in [23]. The size of the image is 128×128. (a) Original SAR image. (b) Initialization for our proposed method. (c) Segmentation by our method. (d) Segmentation by the method in [23]. (e) Magnitude of the level set function in a converged stage by our method. (f) Magnitude of the level set function in a converged stage by the method in [23]

Fig. 2 (a) shows the absolute mean of ϕ. It can be seen that after 20 iterations the absolute mean starts to rise slightly. Fig. 2 (b) shows the absolute mean of $\Delta\phi$, which reflects the magnitude of the control signal. The value is tending towards stability over 15 iterations. Fig. 2 (c) shows the MAMS values after 19 iterations, which is calculated by every latest 19 AM values of $\Delta\phi$, and MAMS is decreasing consistently. The value of MAMS is smaller than the threshold preset after 35 iterations. Hence the evolution can be terminated.

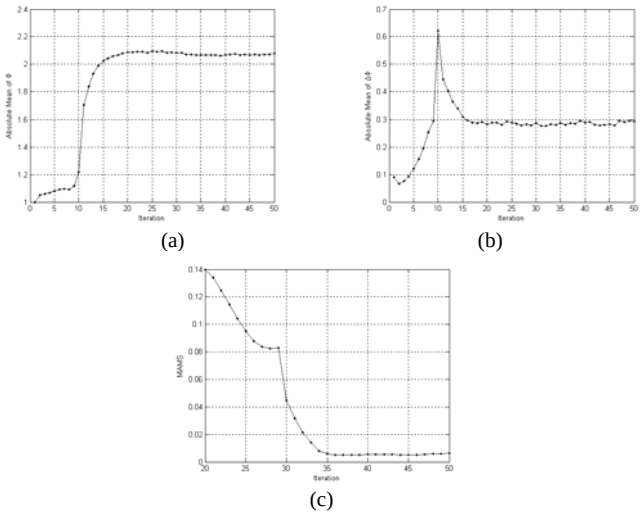

Figure 2. Fig. 2 The criterion of the evolution. (a) The absolute mean of ϕ. (b) The absolute mean of $\Delta\phi$. (c) MAMS.

Fig. 3 shows the segmentation results on two different real SAR images. The salient region is separated and the region boundary is fairly smooth.

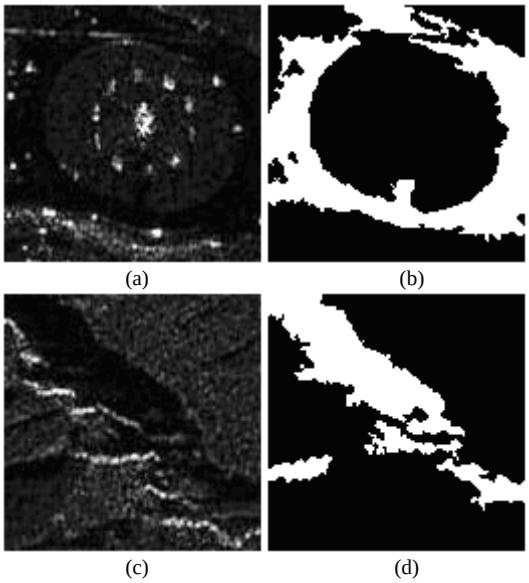

Figure 3. Segmentation results of other SAR images, whose sizes are 128×128. (a) and (c) are the original SAR images, (b) and (d) are the segmentation results of (a) and (c) respectively.

VI. CONCLUSIONS

We have modified the level-set based energy functional that introduced in [23], which is more objective for the purpose of SAR image segmentation. The existence of a global minimum guarantees that the desire segmentation results can be captured. In addition, a convex check factor is employed during the level set evolution process, which can effectively improve the regularity of the result. Moreover we can find our method

is much more robust for getting the desired segmentation result by the comparison between the proposed method and the method proposed in [23]. And the convergence of the absolute mean of $\Delta\phi$ makes it possible to set a reasonable termination criterion without any additional computation. This ensures that the algorithm can be terminated automatically, as the desired result is obtained.

REFERENCES

[1] Canny J F. A computational approach to edge detection. IEEE Trans Pattern Anal Mach Intell, 1986, 8 (6): 679—698

[2] Chen C W, Luo J B, Parker K J. Image segmentation via adaptive k-mean clustering and knowledge-based morphological operations with biomedical applications. IEEE Trans Image Processing, 1998, 7 (12): 1673—1683

[3] Comaniciu D, Meer P. Mean shift: a robust approach toward feature space analysis. IEEE Trans Pattern Anal Mach Intell, 2002, 24 (5): 603—619

[4] Comaniciu D, Meer P. Mean shift analysis and applications. Proc IEEE International Conference on Computer Vision (ICCV'99), Kerkyra, Greece, 1999. 1197—1203

[5] Carvalho E A, Ushizima D M, Medeiros F N S, et al. SAR imagery segmentation by statistical region growing and hierarchical merging. Digital Signal Processing, 2010, 20: 1365—1378

[6] Bernad G P, Denise L, Réfrégier P. Hierarchical feature-based classification approach for fast and user-interactive SAR image interpretation. IEEE Trans Goesci Remote Sens Lett, 2009, 6(1): 117—121

[7] White R G. Change detection in SAR imagery. Int J Remote Sens, 1991, 12 (2): 339—360

[8] Frulla J L L. An automated region growing algorithm for segmentation of texture regions in SAR images, 1998 Int J Remote Sens, 1998,19(18): 3595—3606

[9] Yu Q, Clausi D A. SAR sea-ice image analysis based on iterative region growing using semantics. IEEE Trans Goesci and Remote Sens, 2007, 45 (12): 3919—3931

[10] Yu Q, Clausi D A. IRGS: image segmentation using edge penalties and region growing. IEEE Trans Pattern Anal Mach Intell, 2008, 30 (12): 2126—2139

[11] Nicolas J M, Tupin F, Maitre H. Smoothing speckled SAR images by using maximum homogeneous region filters: an improved approach. IEEE International Geoscience and Remote Sensing Symposium (IGRSS'01), 2001. 1503—1505

[12] Hua X, Pierce L E, Ulaby F T. SAR speckle reduction using wavelet denoising and markov random field modeling. IEEE Tran Goesci Remote Sens, 2002, 40 (10): 2196—2212

[13] Park J M, Song W J, Pearlman W A. Speckle filtering of SAR images based on adaptive windowing. IEE Proceedings on Vision, Image and Signal Processing, 1999. 191—197

[14] Frost V S, Shanmugan K S, Holtzman J C. A model for radar images and its application to adaptive filtering of multiplicative noise. IEEE Trans Pattern Anal Mach Intell, 1982, 4(2): 157—166

[15] Gao G, Zhao L, Zhang J, et al. A segmentation algorithm for SAR images based on the anisotropic heat diffusion equation. Pattern Recognition, 2008, 41: 3035—3043

[16] Ayed I B, Vazquez C, Mitiche A, et al. SAR image segmentation with active contours and level sets. Proc IEEE International Conference on Image Processing (ICIP'04), Singapore, 2004. 2717—2720

[17] Ayed I B, Mitiche A, Belhadj Z. Multiregion level-set partitioning of synthetic aperture radar images. IEEE Trans Pattern Anal Mach Intell, 2005, 27 (5): 793—800

[18] Chan T, Vese L. Active contours without edges. IEEE Trans Image Processing, 2001, 10 (2): 266—277

[19] Mansouri A R, Mitiche A, Vazquez C. Image partitioning by level set multiregion competition. Proc IEEE International Conference on Image Processing (ICIP'04), Singapore, 2004. 2721—2724

[20] Germain O, Réfrégier P. Edge location in SAR images: performance of the likelihood ratio filter and accuracy improvement with an active contour approach. IEEE Trans Image Processing 2001, 10(1): 72—78

[21] Chesnaud C, Refregier P, Boulet W. Statistical region snake-based segmentation adapted to different physical noise models. IEEE Trans Pattern Anal Mach Intell, 1999, 21(11): 1145—1157

[22] Kass M, Withkin A, Terzopoulos D. Snakes: actives contours model. International Journal on Computer Vision, 1998, 1 (1) 321—333

[23] Shuai Y, Sun H, Xu G. SAR image segmentation based on level set with stationary global minimum. 2008 IEEE Trans Goesci Remote Sens Lett, 2008, 5 (4): 644---648

[24] Zhu S C, Yuille A. Region competition: unifying snakes, region growing, and Bayes/MDL for multiband image segmentation, IEEE Trans Pattern Anal Mach Intell, 1996, 18 (9): 884—900

Qiangqiang Peng is born in Ningxia province in Apr. 1984. He received his B.S. degree and M.S. degree form Northeastern University, Shenyang, China and North China University of Technology, Beijing, China in 2006 and 2009 respectively. His research interest is on SAR imagery modeling and processing.

He is currently a candidate of Ph.D. in Control Theory and Control Engineering in Beihang University, Beijing, China.

Long Zhao is born in Inner Mongolia province in Jan. 1976. he received his Ph.D. in Precision Instrument and Machinery in 2004 from Beijing University of Aeronautics and Astronautics , Beijing, China. Prior to that, he received a B.S. degree in Control Theory and Control Engineering in 2001 from Harbin Engineering University, Harbin, China and an M.S. degree in Mathematics Education in 1998 from Inner Mongolia Normal University, Inner Mongolia, China.

He is currently an associate professor in the School of Automation Science and Electrical Engineering at Beihang University, Beijing, China. He is the leader of the Digital Navigation Center at Beihang University. His research focuses on the terrain aided navigation and their integration with other enabling navigation system.